Quantitative modeling of bubble competition in Richtmyer-Meshkov instability

Sung-Ik Sohn*
Department of Mathematics, Kangnung National University, Kangnung 210-702, Korea
(Received 27 March 2008; published 3 July 2008)

We present a quantitative model for the evolution of single and multiple bubbles in the Richtmyer-Meshkov (RM) instability. The higher-order solutions for a single-mode bubble are obtained, and distinctions between RM and Rayleigh-Taylor bubbles are investigated. The results for multiple-bubble competition from the model shows that the higher-order correction to the solution of the bubble curvature has a large influence on the growth rate of the RM bubble front. The model predicts that the bubble front of RM mixing grows as $h \sim t^{\theta}$ with $\theta \sim (0.3-0.35) \pm 0.02$.

DOI: 10.1103/PhysRevE.78.017302 PACS number(s): 47.20.Ma, 47.20.Ky

An interface between two fluids of different density accelerated by a shock wave is hydrodynamically unstable. This instability is known as the Richtmyer-Meshkov (RM) instability [1]. The RM instability plays important roles in many fields, ranging from astrophysics to inertial confinement fusion, and has many common features with the Rayleigh-Taylor (RT) instability [2,3], which is driven by a gravitational acceleration. Since Richtmyer [1] first considered this problem, it has received attention in a wide range of contexts, but many aspects of dynamics of the instability are still uncertain.

The main purpose of this paper is to present a quantitative model for both single- and multiple-bubble evolution in the RM instability. Theoretical models for comprehensive descriptions of the motion of bubbles are the potential flow models proposed by Layzer [4] and Zufiria [5]. The key difference between the two models is that the velocity potential in the Layzer model is an analytical function of sinusoidal form, while in the Zufiria model it has a point source. The Layzer and Zufiria models were originally developed for the RT instability, and were applied to the RM instability by several authors [6–12].

The Layzer and Zufiria models succeeded in the prediction of the velocity of a single-mode bubble in RT and RM instabilities, but there were relatively large differences in the bubble curvature between solutions of the models and numerical results. Moreover, issues such as the dependence of the bubble curvature on the density ratio, and the size of a RM bubble relative to a RT bubble, are not fully clarified yet.

The author recently extended the Zufiria model to multiple-bubble evolution of a RT instability of finite density ratio [13]. One might expect that the model can be applied to the RM instability with no difficulty. However, we have found a surprising result: the Zufiria model in Ref. [13] gives much higher growth rates for multiple bubbles in a RM instability than the numerical and experimental results. We will show that this discrepancy is due to the sensitiveness of the RM bubble competition to the curvature, and that a quantitative prediction for the bubble curvature is critically important in the RM instability.

In this paper, we present a higher-order Zufiria model to give quantitatively correct solutions for single- and multiple-bubble evolution. Using the model, we investigate the differences of a single-mode RM bubble from a RT bubble, and the dynamics of the RM bubble competition.

We consider an interface in a vertical channel filled with two fluids of different density in two dimensions. The densities of the upper and lower fluids are denoted as ρ_1 and ρ_2, respectively. The interface in the vicinity of the bubble tip can be written as

$$\eta(\hat{x},\hat{y},t) = \hat{x} + \sum_{j=1}^{\infty} \zeta_j(t)\hat{y}^{2j} = 0. \tag{1}$$

The frame of reference $(\hat{x},\hat{y})$ moves with the bubble tip with the velocity U. We here take the approximation of the interface (1) up to fourth order in $\hat{y}$. The bubble curvature is denoted as $\xi=-2\zeta_1$.

The potentials of the fluids in the Zufiria model are taken as

$$W_1(\hat{z}) = Q_1 \ln(1 - e^{-k(\hat{z}+H)}) - U\hat{z}, \tag{2}$$

$$W_2(\hat{z}) = Q_2 \ln(1 - e^{-k(\hat{z}-H)}) + (K-U)\hat{z}, \tag{3}$$

where $k=2\pi/L$ is the wave number, and L the channel width. The evolution of the bubble is determined by the kinematic condition and the Bernoulli equation. The derivation of higher-order equations for the Zufiria model is similar to the low-order case [12,13], and thus only the resulting equations are given below.

Using Eqs. (1)–(3) and satisfying the kinematic condition up to fourth order in $\hat{y}$, we have

$$U = c_1 Q_1 = \tilde{c}_1 Q_2 + K, \tag{4}$$

$$\frac{d\zeta_1}{dt} = Q_1\left(3c_2\zeta_1 + \frac{c_3}{2}\right) = Q_2\left(3\tilde{c}_2\zeta_1 + \frac{\tilde{c}_3}{2}\right), \tag{5}$$

$$\frac{d\zeta_2}{dt} = Q_1\left(5c_2\zeta_2 - \frac{5}{2}c_3\zeta_1^2 - \frac{5}{6}c_4\zeta_1 - \frac{c_5}{24}\right) = Q_2\left(5\tilde{c}_2\zeta_2 - \frac{5}{2}\tilde{c}_3\zeta_1^2 - \frac{5}{6}\tilde{c}_4\zeta_1 - \frac{\tilde{c}_5}{24}\right). \tag{6}$$

The second- and fourth-order equations in $\hat{y}$ of the Bernoulli equation are

*sohnsi@kangnung.ac.kr

$$\left(c_1\zeta_1+\frac{c_2}{2}\right)\frac{dQ_1}{dt}+Q_1\left(c_2\zeta_1+\frac{c_3}{2}\right)\frac{dH}{dt}-\frac{1}{2}Q_1^2c_2^2+g\zeta_1$$
$$=\mu\left[\left(\tilde{c}_1\zeta_1+\frac{\tilde{c}_2}{2}\right)\frac{dQ_2}{dt}+\zeta_1\frac{dK}{dt}-Q_2\left(\tilde{c}_2\zeta_1+\frac{\tilde{c}_3}{2}\right)\frac{dH}{dt}\right.$$
$$\left.-\frac{1}{2}Q_2^2\tilde{c}_2^2+g\zeta_1\right], \tag{7}$$

$$\left(\frac{c_2}{2}\zeta_1^2+\frac{c_3}{2}\zeta_1+\frac{c_4}{24}-c_1\zeta_2\right)\frac{dQ_1}{dt}$$
$$+Q_1\left(\frac{c_3}{2}\zeta_1^2+\frac{c_4}{2}\zeta_1+\frac{c_5}{24}-c_2\zeta_2\right)\frac{dH}{dt}+G_1$$
$$=\mu\left[\left(\frac{\tilde{c}_2}{2}\zeta_1^2+\frac{\tilde{c}_3}{2}\zeta_1+\frac{\tilde{c}_4}{24}-\tilde{c}_1\zeta_2\right)\frac{dQ_2}{dt}\right.$$
$$\left.-Q_2\left(\frac{\tilde{c}_3}{2}\zeta_1^2+\frac{\tilde{c}_4}{2}\zeta_1+\frac{\tilde{c}_5}{24}-\tilde{c}_2\zeta_2\right)\frac{dH}{dt}+G_2\right],$$

$$G_1=\frac{Q_1^2}{2}\left(c_2^2\zeta_1^2-c_2c_3\zeta_1+\frac{c_3^2}{4}-\frac{c_2c_4}{3}\right)-g\zeta_2,$$

$$G_2=\frac{Q_2^2}{2}\left(\tilde{c}_2^2\zeta_1^2-\tilde{c}_2\tilde{c}_3\zeta_1+\frac{\tilde{c}_3^2}{4}-\frac{\tilde{c}_2\tilde{c}_4}{3}\right)-g\zeta_2, \tag{8}$$

where $\mu=\rho_2/\rho_1$ denotes the density ratio. The external acceleration g is set to 0 for the RM instability. The expressions for $c_i(H)$ are given in Ref. [13], and $\tilde{c}_i(H)=c_i(-H)$. Equations (4)–(8) determine the dynamics of a bubble of finite density contrast. Note that Eq. (6) is a new equation, and Eqs. (4), (5), (7), and (8) are the same as in the low-order model [12], except for the terms with ζ_2 in Eq. (8).

One can check that Eqs. (4)–(8) remain the same even after retaining higher-order terms than the fourth order in $\hat{y}$, and thus expansion higher than fourth order is not needed in the Zufiria model. Usually, in other models, a higher-order expansion contributes a corresponding correction to the bubble velocity and curvature [7,9,11,14]. This is a crucial difference of the Zufiria model from other theoretical models, and explains why the present model provides accurate predictions for the bubble motion.

The asymptotic solution for a bubble in the RM instability from the higher-order model is

$$\zeta_1\to\frac{k(\lambda+1)}{6(\lambda-1)},\quad \zeta_2\to\frac{k^3(\lambda^3+\lambda^2+\lambda+1)}{180(\lambda-1)^3},$$

$$H\to\frac{1}{k}\ln\lambda,\quad Q_1\sim\frac{(\lambda-1)^2[(A+3)\lambda-2A]}{3(1+A)\lambda^2k^2t},$$

$$U\sim\left(\frac{A+3}{3(1+A)}-\frac{1}{\lambda}+\frac{2A}{3(1+A)\lambda^2}\right)\frac{1}{kt},\quad K\to U, \tag{9}$$

where λ is the root, larger than 1, of a cubic polynomial

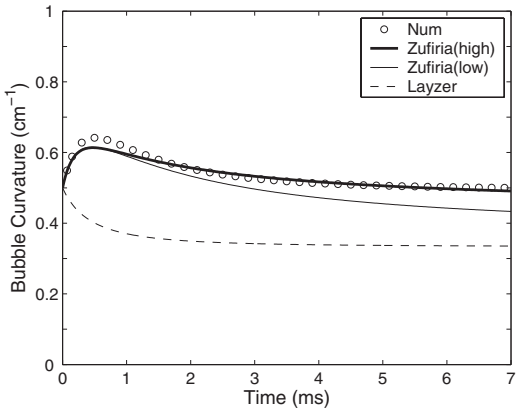

FIG. 1. Curvature of a single-mode bubble. The Atwood number is $A=0.7$.

$$p(\lambda)=(18-2A)\lambda^3-(102+42A)\lambda^2$$
$$+(18+78A)\lambda-17A+3,$$

and A is the Atwood number, defined as $A=(\rho_1-\rho_2)/(\rho_1+\rho_2)$. One can find that the root $\lambda(A)$ of this polynomial is an increasing function of the Atwood number, having the values 5.479 at $A=0$ and 8.289 at $A=1$. The asymptotic curvature of a RM bubble thus ranges from $0.482k$ for $A=0$ to $0.425k$ for $A=1$. The low-order model predicted that the asymptotic bubble curvature of RM instability varied from $0.447k$ to $0.383k$ with respect to A. Therefore, the correction factor of the curvature to the low-order solution is 10%.

A comparison of the solution of the RM instability with that of the RT instability is an interesting and important issue. The asymptotic solution for a RT bubble from the higher-order model can be obtained by setting the external acceleration $g=$const, and is given by

$$\zeta_1\to\frac{k(\lambda+1)}{6(\lambda-1)},\quad U\to\frac{\sqrt{\lambda^2-1}}{\lambda}\sqrt{\frac{2Ag}{3(1+A)k}}. \tag{10}$$

Here, λ is the root, larger than 1, of a polynomial $p(\lambda)=7\lambda^2-40\lambda+7$. From Eq. (10), the asymptotic bubble curvature is $0.480k$, independent of the density ratio.

The higher-order solutions (9) and (10) give a different conclusion for the bubble curvature from the low-order model [12]. The low-order model predicted that the asymptotic bubble curvature of RT instability was $0.577k$, independent of the density ratio. In the low-order model, the asymptotic curvature of a RM bubble was smaller than that of a RT bubble over all Atwood numbers, fixing the wave number, and the quantitative difference of the asymptotic curvature between two instabilities was relatively large. However, their difference gets smaller after the higher-order correction, and even for small Atwood numbers, the asymptotic curvature of a RM bubble is nearly the same as that of a RT bubble.

In Fig. 1, we compare the finite-time solutions for the bubble curvature of the RM instability from the low- and higher-order Zufiria models with the result of full numerical simulations [15], and a solution of the Layzer-type model [9]. The finite-time solutions of the models are obtained by

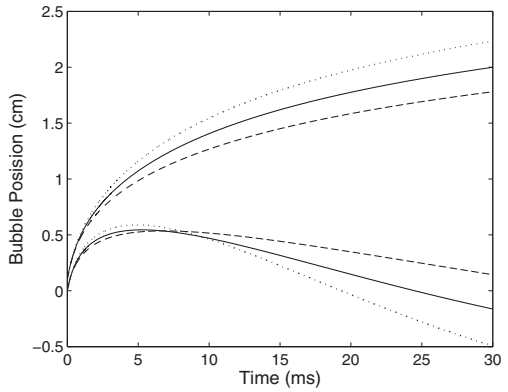

FIG. 2. Bubble position for $N=3$ for selected Atwood numbers. The dashed curves correspond to $A=0.9$, the solid curves to $A=0.5$, and the dotted curves to $A=0.2$.

integrating the equations numerically. The Atwood number is $A=0.7$ and the channel width $L=2\pi$ cm. The initial amplitude and velocity of the interface are 0.5 cm and 0.8 cm/ms, respectively. In Fig. 1, we find an excellent agreement of the solution of the higher-order model with the numerical result. We will show that, although the solution from the low-order model is reasonably good for the single-mode case, the correction for the bubble curvature from the higher-order model gives completely different results for multiple bubbles in the RM instability. In Fig. 1, we also see that the solution of the Layzer model has a large difference from the numerical result. The prediction of the Layzer model may be slightly improved by adding higher-order terms in the equations, as demonstrated by Goncharov [9] for $A=1$. Note that a higher-order Layzer model for $A<1$ has not been developed yet.

There are some contradictory predictions for the bubble growth among theoretical models. The multiple harmonic model by Abarzhi *et al.* [11] predicts that the asymptotic bubble velocity in the RM instability is $U\sim 3/Akt$, which strongly depends on the Atwood number, and the bubble curvature asymptotically tends to zero, contrary to the results of the Zufiria and Goncharov models. The numerical results [6,15] show that the asymptotic bubble velocity has a weak dependence on the Atwood number and the bubble curvature approaches a finite value at a late time. Abarzhi assumed that the bubble velocity is the fastest solution with respect to the curvature, in order to close the equations, and the generality of this approach may be questionable.

The higher-order model is now extended to multiple-bubble competition of arbitrary density ratio. The channel of width L contains N distinct bubbles and the positions of the bubble tips are $Z_i=X_i+iY_i$, $i=1,2,\ldots,N$, in the laboratory frame of reference. The potential for multiple bubbles can be constructed as the sum of the potential for each bubble [5,13]. Satisfying the kinematic and Bernoulli equations with the potentials, one can derive a $5N$ system of equations. The derivation procedure is similar to the low-order model [13], and the expression for the equations is not given here.

Our model assumes that the bubbles do not move laterally, i.e., $Y_i=$const, neglecting transverse effects due to asymmetry around a bubble. Experimental and numerical observations [6,16] show that, in the bubble competition process, the bubbles move mainly in the longitudinal direction and the lateral motion of the bubbles is negligible.

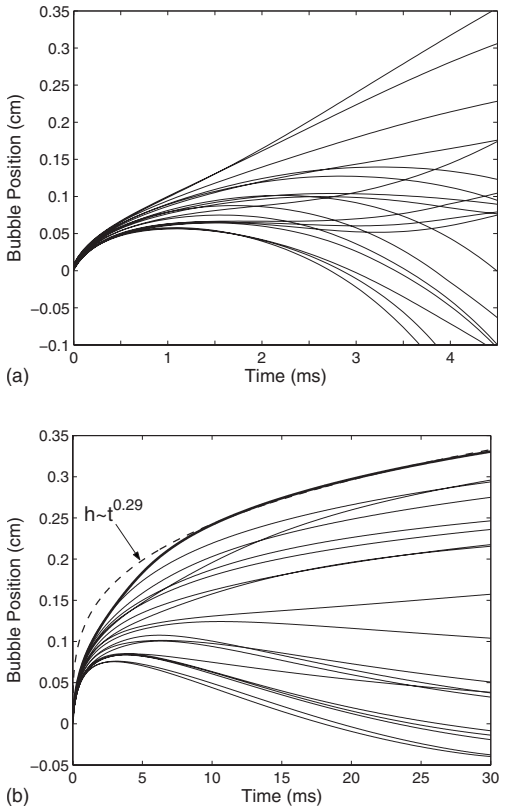

FIG. 3. Bubble position for $N=20$. The Atwood number is $A=0.5$. (a) Low- and (b) higher-order models.

Initially, the bubbles in the channel are equally spaced along the horizontal direction, and the longitudinal positions X_i are perturbed. The initial velocity and curvature of bubbles are scaled as $U_i=U^0/\sqrt{N-1}$, $\xi_i=\xi^0(N-1)$, $i=1,\ldots,N$, where U^0 and ξ^0 are given constants. For all runs in this paper, U^0 is set to 1 cm/ms and ξ^0 to 0.5 cm^{-1}.

The higher-order multiple-bubble model is first applied to the three-bubble interaction as the simplest case. Figure 2 is the result for the bubble position for $N=3$ for selected Atwood numbers. The dashed curves correspond to $A=0.9$, the solid curves to $A=0.5$, and the dotted curves to $A=0.2$. The initial bubble heights are $X_1=X_3=0.1$ cm and $X_2=0$. The first bubble is identical to the third one, by the symmetry of the vertical walls. Figure 2 shows that the initially higher bubbles grow faster than the lower ones, while the lower bubbles advance at early times, and after reaching maxima are washed downstream with constant velocities. We observe that, for smaller density ratio, the front bubble grows faster, and also the lower bubble retreats faster.

Next, we run simulations for $N=20$ bubbles. Figure 3 shows the bubble positions for $A=0.5$ from the low-order and the higher-order models for the same initial conditions. Initially, the longitudinal positions of bubbles X_i are randomly perturbed in the interval [0,0.01] cm. Figure 3(a) shows that the bubble front from the low-order model has a much larger growth rate, unlike the results reported in [16–18]. In Fig. 3(b), we see that the higher-order model makes the growth rate of the bubble front decrease dramati-

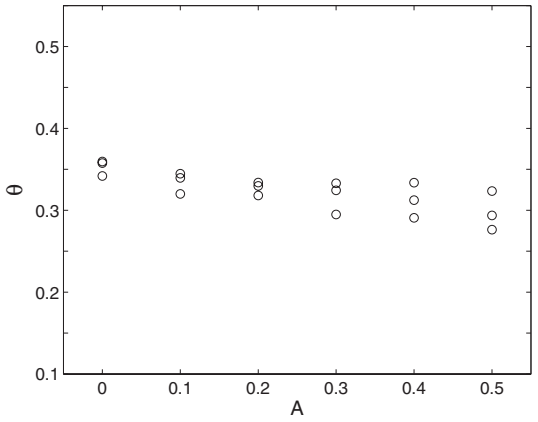

FIG. 4. Growth exponent θ vs the Atwood number.

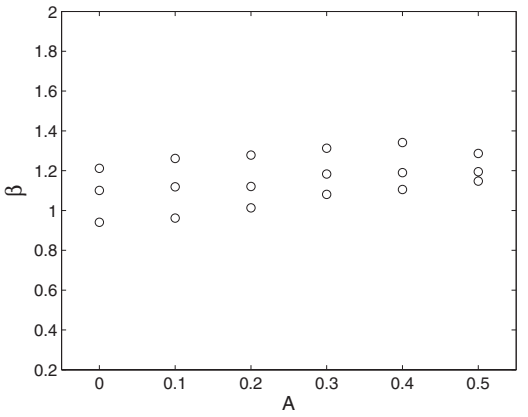

FIG. 5. Self-similarity ratio β vs the Atwood number. The values of β are averages in the scale-invariant regime.

cally. The curve $h=at^{\theta}$ with $a=0.12$, $\theta=0.29$ is fitted to the front bubble. The coefficient and exponent of this curve are calculated by least squares fitting, in the invariant regime of the self-similarity parameter β, which will be defined shortly. Figure 3 shows that the higher-order correction of the bubble curvature has a large influence on the growth rate of the bubble front in a RM instability. This implies that the dynamics of the RM bubble competition are sensitive to the bubble curvature, and a quantitatively accurate prediction for the bubble curvature is essential in the modeling of RM mixing.

Figure 4 shows the result of the higher-order model for the growth exponent θ for the Atwood number $A \leq 0.5$ from several runs with different initial perturbations. The exponent θ in Fig. 4 has a range of $(0.3-0.35) \pm 0.02$. Linear electric motor experiments in three dimensions by Dimonte and Schneider [16] reported $\theta \sim 0.2-0.32$ for $0.1 < A < 0.5$. Full numerical simulations by Oron *et al.* [17] gave $\theta \sim 0.35$ in two dimensions, and $\theta \sim 0.22$ in three dimensions. Thus, our result is in good agreement with the previous results. In Fig. 4, we observe a downward tendency of θ with the Atwood number. This behavior is also found in the results of the drag-buoyancy model [18].

Unfortunately, the higher-order model suffers from a numerical instability for large Atwood numbers. The reason for this instability is not clarified. Simulations of the higher-order model for $A > 0.5$ usually have large oscillations in the solution, or stop in the middle of a run.

The self-similar behavior of the ratio of the bubble diameter to the bubble height is well known in RT mixing [16,17,19]. We examined this ratio for RM mixing, and checked that the RM bubbles indeed grow self-similarly with the aspect ratio. Figure 5 is the average of the ratio $\beta = 2\bar{R}/h$ in the scale-invariant regime with respect to the Atwood number, where $\bar{R}$ is defined as the average radius of curvatures of bubbles with positive velocities. In Fig. 5, we see that the model gives $\beta \sim (1-1.3) \pm 0.05$ for $A \leq 0.5$. To the author's knowledge, there is no other published result for the aspect ratio β in RM mixing. Oron *et al.* [17] assumed that the parameter β for RM mixing is similar to that for RT mixing. For the case of RT mixing, the result for β is about 0.4–0.6 [13,16]. Therefore, Fig. 5 shows that the similarity parameter β for the RM mixing is twice larger than the RT mixing.

We also run the simulations for $N=40$ bubbles. The results of the $N=40$ runs for the growth exponent and the aspect ratio were $\theta \sim 0.3-0.38$ and $\beta \sim 1.1-1.27$ for $A \leq 0.5$. The growth exponent from $N=40$ runs is nearly the same as for $N=20$, and the aspect ratio has a narrower range.

In conclusion, the results from the present model showed the critical importance of quantitative prediction for the bubble curvature in the RM instability. It is found that the growth exponent α and the aspect ratio β exhibit opposite slopes with the Atwood number, but are overall insensitive to the density ratio.

This work was supported by the Korea Research Foundation funded by the Korean Government (MOEHRD) under Grant No. KRF-2007-013-C00008.

[1] R. D. Richtmyer, Commun. Pure Appl. Math. **13**, 297 (1960).
[2] D. Sharp, Physica D **12**, 3 (1984).
[3] G. I. Taylor, Proc. R. Soc. London, Ser. A **201**, 192 (1950).
[4] D. Layzer, Astrophys. J. **122**, 1 (1955).
[5] J. Zufiria, Phys. Fluids **31**, 440 (1988).
[6] J. Hecht *et al.*, Phys. Fluids **6**, 4019 (1994); U. Alon *et al.*, Phys. Rev. Lett. **74**, 534 (1995).
[7] N. A. Inogamov, Sov. Phys. JETP **80**, 890 (1995); N. A. Inogamov, Laser Part. Beams **15**, 53 (1997).
[8] Q. Zhang, Phys. Rev. Lett. **81**, 3391 (1998).
[9] V. N. Goncharov, Phys. Rev. Lett. **88**, 134502 (2002).
[10] K. O. Mikaelian, Phys. Rev. E **67**, 026319 (2003).
[11] S. I. Abarzhi, K. Nishihara, and J. Glimm, Phys. Lett. A **317**, 470 (2003).
[12] S.-I. Sohn, Phys. Rev. E **70**, 045301(R) (2004).
[13] S.-I. Sohn, Phys. Rev. E **75**, 066312 (2007).
[14] N. Zabusky *et al.*, J. Fluid Mech. **475**, 147 (2003).
[15] S.-I. Sohn, Phys. Rev. E **69**, 036703 (2004).
[16] G. Dimonte and M. Schneider, Phys. Fluids **12**, 304 (2000).
[17] D. Oron *et al.*, Phys. Plasmas **8**, 2883 (2001).
[18] G. Dimonte, Phys. Plasmas **7**, 2255 (2000).
[19] J. Glimm and D. H. Sharp, Phys. Rev. Lett. **64**, 2137 (1990).